Materials Letters 171 (2016) 255–258

Contents lists available at ScienceDirect

Materials Letters

journal homepage: www.elsevier.com/locate/matlet

Solid-state synthesis of $CuBi_2O_4$/MWCNT composites with enhanced photocatalytic activity under visible light irradiation

Minmin Chen [a], Qingya Yang [a], Longfeng Li [a,b,*], Mingzhu Liu [a], Peipei Xiao [a], Maolin Zhang [a,b,*]

[a] School of Chemistry and Materials Science, Huaibei Normal University, Huaibei 235000, PR China
[b] Information College, Huaibei Normal University, Huaibei 235000, PR China

ARTICLE INFO

Article history:
Received 22 January 2016
Received in revised form
18 February 2016
Accepted 21 February 2016
Available online 23 February 2016

Keywords:
Composite materials
Semiconductors
Structural
$CuBi_2O_4$
Photocatalyst

ABSTRACT

A novel $CuBi_2O_4$/multiwalled carbon nanotube ($CuBi_2O_4$/MWCNT) composite was facilely synthesized via a ball-milling process for 2 h at room temperature for the first time. The structure, morphology and composition were characterized with powder X-ray diffraction (XRD) and transmission electron microscopy (TEM). The photocatalytic activity was evaluated by a degradation experiment. The results showed that the $CuBi_2O_4$ with nanorod structure was well deposited on MWCNT, and the $CuBi_2O_4$/MWCNT composites exhibited higher photocatalytic activity than pure $CuBi_2O_4$. Among the developed composites, 20 wt% MWCNT incorporated $CuBi_2O_4$ composite displayed optimal photocatalytic activity for degradation of methyl orange (MO) under visible light irradiation in comparison to pure $CuBi_2O_4$ and other composites. The synergistic coupling effect between the $CuBi_2O_4$ and MWCNT contributed to the superior performance of the novel $CuBi_2O_4$ composites.

1. Introduction

Synthetic textile dyes and other industrial dyestuffs are among the largest groups of water pollutants in the world. Removing these non-biodegradable dye molecules from the environment is a crucial ecological problem due to their toxicity and potential carcinogenicity [1]. Semiconductor-based photocatalytic technology is required for the removal of dyes in order to overcome the drawbacks of conventional physical techniques [2]. Among various semiconductor-based photocatalysts reported recently, $CuBi_2O_4$ is a novel photocatalytic material that is utilized towards dye degradation [3].

However, pure $CuBi_2O_4$ exhibits poor photocatalytic performance under visible and UV light illumination due to its high photostability, great pristine surface and lack of chemical affinity with substrate ions [3–5]. To improve the photocatalytic performance of $CuBi_2O_4$, integration with any promoters such as carbon sources [3], noble metal [6] and semiconductors [7–10] etc., are essential. Among the carbon sources, multi-walled carbon nanotube (MWCNT) has been considered as a promising material owing to its high chemical stability, tubular structure and good adsorption capacity [11]. Besides, MWCNT has been considered as electron sinks, hindering the photogenerated carrier recombination [12]. Fabricating MWCNT-based hybrid photocatalysts have attracted special interest in field of the pollutants photodecomposition. It is believed that there is a synergetic effect between the MWCNT and the semiconductors, improving their photocatalytic performance [11,12].

Taking these into account, we first synthesized $CuBi_2O_4$/MWCNT nanocomposites via a ball-milling assisted solid-state method, and tested it in degradation of methyl orange (MO) solution under visible light irradiation. Results showed that the developed composites exhibited better visible light photocatalytic activity than that of the pure materials. Therefore, $CuBi_2O_4$/MWCNT can be deemed as an attractive candidate for the removal of organic pollutant in water.

2. Experimental

First, a certain amount of MWCNT, 1.552 g of $Bi(NO_3)_3 \cdot 5H_2O$, 0.3866 g of $Cu(NO_3)_2 \cdot 3H_2O$ and 1.92 g of NaOH were mixed together, followed by a ball-milling reaction for 2 h at room temperature using the planetary ball-mill (QM-3SP04) at the rotation speed of 480 rpm. Next, the resulting product was washed with deionized water and absolute ethanol for several times, and then dried under vacuum at 60 °C for 8 h to obtain $CuBi_2O_4$/MWCNT composite (marked as CBM). For the preparation of pure $CuBi_2O_4$, the same procedure was followed without MWCNT. In order to

* Corresponding authors at: School of Chemistry and Materials Science, Huaibei Normal University, Huaibei 235000, PR China.
E-mail addresses: lilongfeng@chnu.edu.cn (L. Li), zhangml@chnu.edu.cn (M. Zhang).

http://dx.doi.org/10.1016/j.matlet.2016.02.106
0167-577X/

prepare various CBM composites, different weight percentages of MWCNT (5%, 10%, 15%, 20% and 25%) were used and were termed as CBM5, CBM10, CBM15, CBM20 and CBM25, respectively.

The crystal structure was examined by powder XRD (Bruker D8 Advance) operating under 40 kV and 40 mA with the X-ray source of Cu-Kα (λ=0.15418 nm), the morphology was observed by TEM (JEM-2100), and the optical property was measured by UV–Vis diffuse reflectance spectroscopy (Beijing Purkinje TU-1901).

Photocatalytic evaluation was performed in a reactor containing 0.1 g of dried CBM powder and 100 mL of MO dye solution (10 mg L^{-1}) at ambient temperature in air under a 300 W Xe lamp with a 420 nm UV cutoff filter. To avoid the experimental errors caused by the adsorption behavior of MO on photocatalysts, the adsorption performance of MWCNT to MO was examined at room temperature by adding 0.1 g MWCNT to 100 mL of 10 mg L^{-1} MO solution under vigorous stirring condition. The result showed that the adsorption equilibrium between MWCNT and MO was reached within 30 min and the adsorptive capacity of MWCNT was ca. 7.3 mg/g. Therefore, prior to irradiation, the resultant solution was stirred for approximately 30 min in the dark to ensure the adsorption–desorption equilibrium between the catalyst and MO molecules. Next, the resultant solution was exposed to light irradiation under magnetic stirring, and a 5.0 mL suspension was withdrawn and centrifuged to separate the catalyst at a given time interval. Finally, MO concentrations were determined by measuring the absorption at the maximum absorption wavelength of MO (464 nm). The degradation efficiency of MO was calculated according to the final and initial concentration of MO in the solutions (c/c_0). Catalytic activity of CBM composites was compared with that of pure $CuBi_2O_4$.

3. Results and discussion

3.1. Structural characterization

Fig. 1 displays the XRD patterns of the MWCNT, $CuBi_2O_4$ and various CBM composites. It demonstrates that MWCNT has two typical diffraction peaks at a 2θ value of 26.603, 44.669 assigned to (004) and (102). Meanwhile, $CuBi_2O_4$ shows prominent peaks at (28.086), (33.356) and (46.798), which separately correspond to planes (211), (310) and (411), in accordance with PDF#79-1810 $CuBi_2O_4$. In addition, CBM composites with different MWCNT contents show similar diffraction peaks to that of $CuBi_2O_4$, and no diffraction peak of MWCNT appears in the composite. The reason is probably attributed to the relatively low content of MWCNT in the different composites and relatively weak diffraction peak of the MWCNT. The average crystallite sizes of $CuBi_2O_4$ in CBM composites calculated from Scherrer's equation are ca. 43, 39, 36, 33 and 31 nm corresponding to CBM5, CBM10, CBM15, CBM20 and CBM25, respectively, indicating that the amount of MWCNT in CBM composites significantly affects the average crystallite sizes of $CuBi_2O_4$, and the average crystallite sizes of $CuBi_2O_4$ gradually decreased with the increase of MWCNT content. It can be explained that the MWCNT in the composites serves as a dispersing template and restricts the transport and growth of $CuBi_2O_4$ nanoparticles.

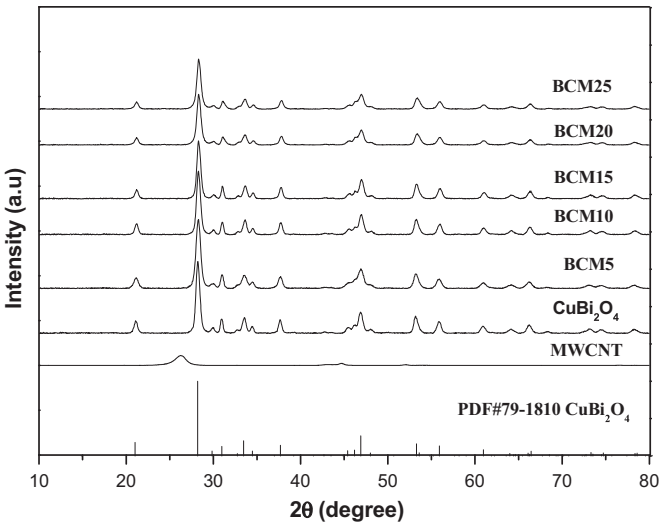

Fig. 1. XRD patterns of the MWCNT, $CuBi_2O_4$ and CBM samples.

Fig. 2a and b demonstrate the morphology and microstructure of pure MWCNT and CBM20 composite. The morphology of pure MWCNT is found to be of tubular structure, whose outer diameter is ca. 10–20 nm (Fig. 2a). And the $CuBi_2O_4$ exhibits the short rod-like structure with ca. 30–40 nm in length (Fig. 2b). Besides, the $CuBi_2O_4$ nanorods are attached on the surface of MWCNT with a little agglomeration.

3.2. Photocatalytic performance

The photocatalytic activities of pure MWCNT, as-synthesized $CuBi_2O_4$ and CBM samples are evaluated by the degradation of MO under visible-light irradiation. Fig. 3 illustrates that the degradation of MO by different photocatalysts. As shown, the photolysis of MO is negligible in the absence of any photocatalyst. And pure MWCNT exhibits a photocatalytic degradation efficiency of 6% for MO after 90 min of visible light irradiation, indicating pure MWCNT has almost no visible light photocatalytic activity. Besides, all CBM composites exhibit higher photocatalytic activity than pure $CuBi_2O_4$, and the degradation efficiency rate of MO slightly increases with an increasing in the amount of MWCNT in CBM nanocomposites from 5 wt% to 20 wt%, indicating that the MWCNT content has a significant influence on the photocatalytic degradation of MO, and the 20 wt% MWCNT sample (CBM20) exhibits optimal photocatalytic ability with the highest degradation efficiency rate of 85% after visible light irradiation for 90 min, which is 2.13 times than that of pure $CuBi_2O_4$. In addition, it is interesting that further increase of the MWCNT content in the composite lead to a decrease of photocatalytic ability compared with CBM20. This is mainly because the superfluous MWCNT covering the surface would prevent $CuBi_2O_4$ from absorbing the light, reducing the total amount of separated carriers. The experimental results confirm that the amount of MWCNT loading plays a major role in the photocatalytic degradation of dyes. In fact, MWCNT incorporated $CuBi_2O_4$ enhances the photocatalytic ability under visible light irradiation due to a positive synergetic effect between the two components including increase in adsorption capacity and reducing photogenerated carrier recombination, which are described as follows: (1) the strong adsorption of MWCNT to MO molecules results in higher concentration of MO molecules on the surface or in the vicinity of $CuBi_2O_4$ deposited on MWCNT, which increases the reaction rate. (2) MWCNT with good electrical conductivity can act as an electron sink and accelerate interfacial charge transfer of CBM photocatalysts, hindering the recombination of photogenerated charge carriers. Thus, the enhanced photocatalytic performance of $CuBi_2O_4$/MWCNT composite can be achieved. In addition, to evaluate photocatalytic activity the absorbed amount of photons in $CuBi_2O_4$ is important. Fig. 4 shows the optical absorption spectra of CBM, $CuBi_2O_4$ and MMWCNT measured by UV–Vis diffuse reflectance spectroscopy. As seen from Fig. 4, the absorption onset of $CuBi_2O_4$ is ca. 794 nm, and its energy band gap is ca.1.56 eV according to the formula $E_g=1240/\lambda$. Also, CBM and MMWCNT have obvious optical absorption in the

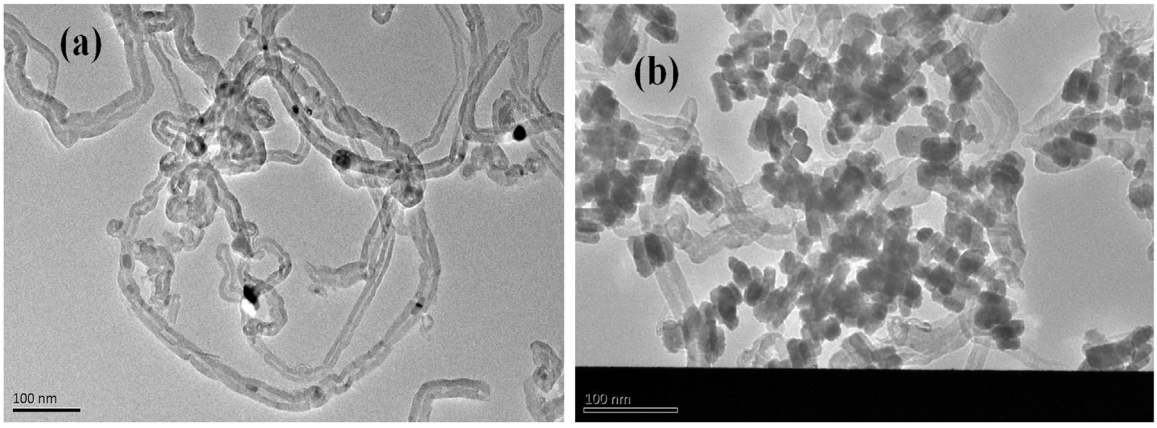

Fig.2. TEM images of (a) pure MWCNT and (b) CBM20 composite.

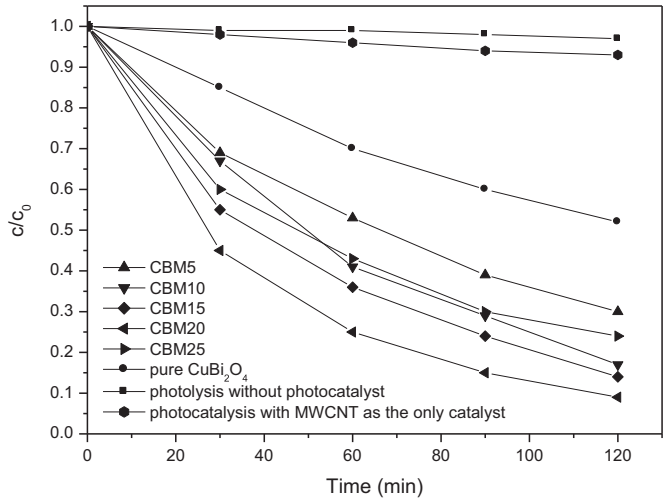

Fig. 3. Photocatalytic activities of $CuBi_2O_4$, MWCNT and CBM with different MWCNT weight percentages under visible-light irradiation.

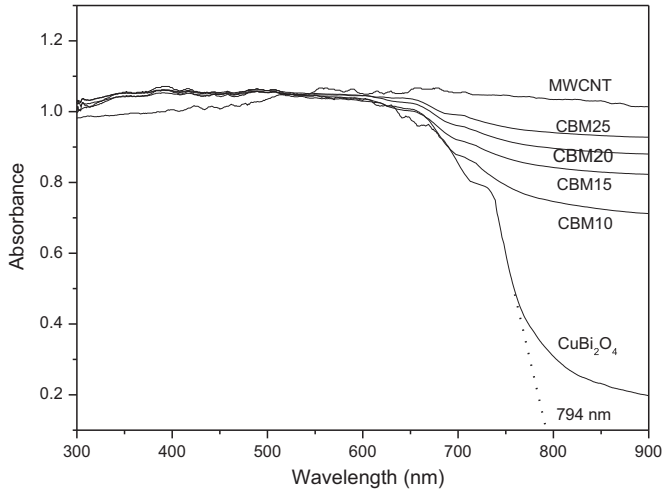

Fig. 4. Optical absorbance spectra of $CuBi_2O_4$, MWCNT and CBM with different MWCNT weight.

UV–visible light region. These absorption spectra provide further evidence that CBM is an effective visible-light-responsive photocatalyst.

4. Conclusion

$CuBi_2O_4$ incorporated MWCNT composites were successfully fabricated by a ball-milling assisted solid-solid reaction approach. The as-fabricated CBM composites exhibited higher photocatalytic activity than pure $CuBi_2O_4$, and CBM 20 showed the highest photocatalytic degradation rate of 85% for MO after visible light irradiation for 90 min. The improved performance of CBM composites was probably ascribed to increase in adsorption capacity and the conductive structure supported by MWCNT, which favors the transfer of photogenerated electrons from the active $CuBi_2O_4$ and promotes the separation of electron–hole pairs.

Acknowledgements

This work is financially supported by the Natural Science Foundation of Anhui Provincial Department of Education (Nos. KJ2014A230 and KJ2016AXXX).

References

[1] S. Malato, P. Fernández-Ibáñez, M.I. Maldonado, J. Blanco, W. Gernjak, Decontamination and disinfection of water by solar photocatalysis: recent overview and trends, Catal. Today 147 (2009) 1–59.
[2] Y. Qu, X. Duan, Progress, challenge and perspective of heterogeneous photocatalysts, Chem. Soc. Rev. 42 (2013) 2568–2580.
[3] Y.H. Xie, Y. Zhang, G.H. Yang, C.H. Liu, J.D. Wang, Hydrothermal synthesis of $CuBi_2O_4$ nanosheets and their photocatalytic behavior under visible light irradiation, Mater. Lett. 107 (2013) 291–294.
[4] E. Abdelkader, L. Nadjia, B. Ahmed, Synthesis, characterization and UV-A light photocatalytic activity of 20 wt%SrO–$CuBi_2O_4$ composite, Appl. Surf. Sci. 258 (2012) 5010–5024.
[5] W.D. Oh, S.K. Lua, Z.L. Dong, T.T. Lim, Rational design of hierarchically-structured $CuBi_2O_4$ composites by deliberate manipulation of the nucleation and growth kinetics of $CuBi_2O_4$ for environmental applications, Nanoscale (2016), http://dx.doi.org/10.1039/C5NR06223C.
[6] S. Anandan, N. Pugazhenthiran, G.J. Lee, J.J. Wu, Photocatalytic degradation of ceftiofur sodium using Au loaded Bi_2CuO_4 nanoparticles, J. Mol. Catal. A: Chem. 379 (2013) 112–116.
[7] T. Arai, M. Yanagida, Y. Konishi, Y. Iwasaki, H. Sugihara, K. Sayama, Efficient complete oxidation of acetaldehyde into CO_2 over $CuBi_2O_4/WO_3$ composite photocatalyst under visible and UV light irradiation, J. Phys. Chem. C 111 (2007) 7574–7577.
[8] Y.Y. Deng, Y.J. Chen, B.G. Chen, J.H. Ma, Preparation, characterization and photocatalytic activity of $CuBi_2O_4/NaTaO_3$ coupled photocatalysts, J. Alloy. Compd. 559 (2013) 116–122.
[9] A. Elaziouti, N. Laouedj, A. Bekka, R.-N. Vannier, Preparation and characterization of p–n heterojunction $CuBi_2O_4/CeO_2$ and its photocatalytic activities under UVA light irradiation, J. King Saud Univ.: Sci. 27 (2015) 120–135.
[10] E. Abdelkader, L. Nadjia, B. Ahmed, Preparation and characterization of novel $CuBi_2O_4/SnO_2$ p–n heterojunction with enhanced photocatalytic performance under UVA light irradiation, J. King Saud Univ.: Sci. 27 (2015) 76–91.
[11] Bo Liu, Z.Y. Li, S. Xu, D.D. Han, D.Y. Lu, Enhanced visible-light photocatalytic

activities of Ag_3PO_4/MWCNT nanocomposites fabricated by facile in situ precipitation method, J. Alloy. Compd. 596 (2014) 19–24.
[12] Z. Wang, L. Yin, M. Zhang, G.W. Zhou, H. Fei, H.X. Shi, H.J. Dai, Synthesis and characterization of Ag_3PO_4/multiwalled carbon nanotube composite photocatalyst with enhanced photocatalytic activity and stability under visible light, J. Mater. Sci. 49 (2014) 1585–1593.